Cure-Induced Phase Separation of Epoxy/DDS/PEK-C Composites and its Temperature Dependency

Xiu-Juan Zhang,[1] Xiao-Su Yi,[2] Yuan-Ze Xu[1]

[1]*Key Laboratory of Molecular Engineering of Polymers, Department of Macromolecular Science, Ministry of Education, Fudan University, Shanghai 200433, China*
[2]*National Key Laboratory of Advanced Composites, Beijing Institute of Aeronautical Materials, Beijing 100095, China*

Received 8 October 2006; accepted 19 January 2008
DOI 10.1002/app.28202
Published online 2 May 2008 in Wiley InterScience (www.interscience.wiley.com).

ABSTRACT: The cure-induced phase separation approach for thermoplastic toughened thermosets of epoxy/DDS (4,4′-diaminodiphenyl sulfone)/PEK-C (modified polyetherketone) is studied by *in situ* rheology, real-time TOM (transmission optical microscope) in wide time–temperature space. Rheology studies show that there are two critical gel transformations corresponding to the loose entangled thermoplastic network at the threshold of phase separation and the percolated denser thermosetting network at chemical gelation point, respectively, within broad cure temperature range. The phase separation time may vary by using rheological or morphological methods, but its temperature dependencies can be well described by Arrhenius equation with similar phase separation activation energy E_a(ps). It is found in the present systems that E_a(ps) keeps unchanged with varying PEK-C content and different epoxy monomers, while changes along the stoichiometric ratio of hardener, which presumably affects the chemical environment of the blends. The quantitative description of time/temperature dependence of phase separation is of practical importance for the design of cure paths in processing and optimizing the properties of TP/TS composites. © 2008 Wiley Periodicals, Inc. J Appl Polym Sci 109: 2195–2206, 2008

Key words: cure-induced phase separation; rheology; morphology; time/temperature dependence; phenolphthalein poly(ether ether ketone); epoxy resin

INTRODUCTION

4,4′-Diaminodiphenylsulfone- (DDS) cured tetraglycidyl-4,4′-diaminodiphenylmethane (TGDDM) is increasingly used as a matrix resin for advanced fiber-reinforced composites in the aerospace and aircraft industries.[1–3] However, because of their tightly crosslinked structure, these materials have some undesirable properties such as low toughness and poor crack resistance, which constrain their many end-use applications. Recently, many attempts have been made to modify the brittle TS with high-performance engineering thermoplastics (TPs).[4–6] Various types of TPs such as poly(ether sulfone) (PES),[4,5] poly(ether imide) (PEI),[6] poly(ether ether ketone)[7] have been employed to toughen epoxy resins. The phase separation to generate adequate morphology is a useful approach to achieve high mechanical properties of final composites. Some results indicate that a fine phase-separated structure and good interfacial adhesion between the two separated phases usually yields greater fracture toughness.

The knowledge about the thermodynamics and the kinetics of cure-induced phase separation of TP/TS blends comprise the basis of the morphology design using controlled phase separation in the composite processing time/temperature window. There are extensive literature on temperature-induced phase separation discussing the thermodynamic description of Flory-Huggins interaction for polymer blends[8] and its time evolution based on the theory of viscoelastic phase separation,[9] which describes the morphology development of spinodal or bimodal decomposition in asymmetric mixtures. The detailed analysis on the cure-induced phase separation of the asymmetric TP/TS systems, where the compositions—the thermosetting species with different molar mass—keep changing with reaction, is still required.[10–15]

Furthermore, the processing of the TP/TS blends is always carried out in wide time/temperature space as presented by TTT (time–temperature-transformation) diagram for usual TS curing.[16] For TP/TS blends, to determine the cure path, it is necessary to know the time/temperature dependency of cure-induced phase separation. To date, relatively few

Correspondence to: Y.-Z. Xu (yuanzexu@fudan.edu.cn).
Contract grant sponsor: Major State Basic Research Projects; contract grant number: 2003CB615604.
Contract grant sponsor: National Natural Science Foundation of China; contract grant number: 20490220.
Contract grant sponsor: Shengli Oilfield, SINOPEC.

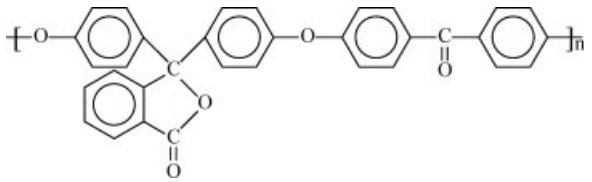

Figure 1 The chemical structure of PEK-C.

studies have been carried out on it in wide time–temperature ranges.[14,15,17,18] Indeed, the usual techniques to trace phase separation, e.g., SALS (small angle light scattering)[10,11] or turbidity are not very efficient in some cases of curing TP/TS blends that have similar refractive index or high transparency upon phase separation, e.g., our present TGDDM/DDS/PEK-C systems. In this work, we will illustrate our rheology, optical microscopy, and thermal approaches on a system of practical importance as follows: TGDDM/DDS/PEK-C, where PEK-C (phenolphthalein poly(ether ether ketone)) is a newly developed high-performance engineering TPs with repeat units as shown in Figure 1:[19]

PEK-C is miscible with epoxy resin in the whole composition range[20,21] and readily yields regular inverted phase structures with size scale $\leq$3 μm. The PEK-C toughened material also shows excellent mechanical properties and fracture toughness.[22] We hope the results of this article will provide an intellectual understanding of the practical cure process of TP/TS composites with phase separation, and shed light on the design of cure paths to optimize the materials properties.

EXPERIMENTAL

Materials and sample preparation

The diglycidyl ether of bisphenol A- (DGEBA) based epoxy resins with epoxide equivalent weight (EEW) of 185 for E54 and 227 for E44 were supplied by Wuxi Synthetic Resin (Jiangsu, China). *N*,*N*,*N*′,*N*′-tetraglycidyl-4,4′-diaminodiphenylmethane (TGDDM) with EEW of 125 was provided by the Shanghai Institute of Synthetic Resins (Shanghai, China). Curing agent DDS with amino hydrogen equivalent weight of 62 was provided by Shanghai Reagent (Shanghai, China). PEK-C (T_g = 221°C, M_w = 108,900) was produced in Xuzhou Engineering Plastics Factory of China.

To prepare the TGDDM/DDS/PEK-C blends, PEK-C was first dissolved in the epoxy monomers (DGEBA was incorporated for better processing and mass ratio of TGDDM/DGEBA is 3/2 throughout the paper unless specified) with continuous stirring at 130°C for about 2 h. Then, DDS was added to the mixture with stoichiometric ratio (except those formulations with particular indication) and stirred vigorously for another 10 min. The obtained transparent homogeneous mixture was stored in refrigerator (about −15°C) for use.

The loading level of PEK-C to epoxy precursors (mixture of epoxy monomer and hardener) is 10, 15, 20, and 30 phr (part per hundred resin), respectively.

Measurements

Dynamic rheological measurement

The rheological experiments were performed using the time-resolved rheometric technique[23] with a rotational rheometer (ARES of TA Instrument), equipped with disposable parallel plates (diameter: 40 mm). The rheometric measurement modes were frequency/temperature sweep (F/T sweep with temperature increment set to zero) under isothermal conditions. The rheometric measurement conditions were as follows: frequency 1, 2, 5, 10, and 20 rad/s, initial strain 5%, and gap 1 mm. The strain was automatically adjusted to maintain the torque response within the limit of the transducer.

The data are split into separated sets (one for each experimental frequency) to follow the evolution with time. Frequency-dependent data can then be interpolated at any given time of the experiment, i.e., at any stage of cure, resulting in ''snapshots'' of intermediate rheological patterns of the cured material, as shown later in Figure 3.

TABLE I
Effect of TOM Magnification on the Phase Separation Time Determination for Epoxy/DDS/PEK-C Systems

PEK-C content (phr)	T (°C)	t_{ps} (1500×) (s)	t_{ps} (1200×) (s)	t_{ps} (760×) (s)	Error (%)
10	210	228	227	220	−1.3–2.2
	200	328	321	320	−0.9–1.5
	190	469	466	464	−0.4–0.6
	180	610	608	602	−0.8–0.5
15	210	200	205	201	−1.0–1.5
	200	287	289	286	−0.3–0.7
	190	399	397	402	−0.5–0.7
	180	589	583	580	0.7–0.9

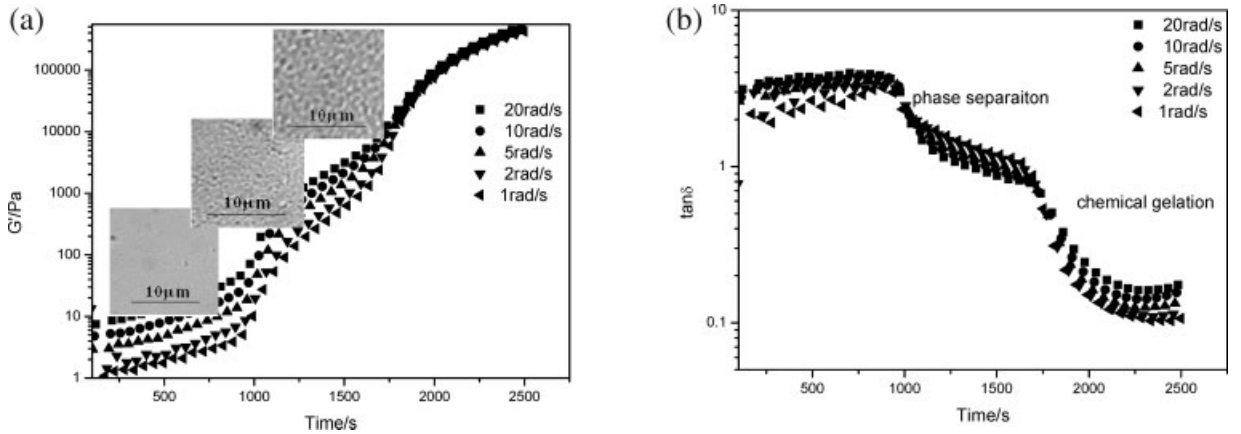

Figure 2 Time evolvements of (a) storage modulus G' and (b) loss tangent tan δ at different frequencies and the morphologies at transitions for epoxy/DDS/PEK-C 15 phr system at 170°C.

TOM

To observe the initial stage of phase separation, a lab-made computerized transmission optical microscope (TOM) system equipped with inversed optical design, long-focusing objective lens, high-temperature controllable hot chamber, and digital image processing system was built up, which allows long-term observation and data collection with a high resolution of 0.2 μm in wide working temperature range of 25–250°C.[17] The system can assign the onset of phase separation for systems with low refractive index difference or systems with domain size as small as 1 μm, which would not be done by usual TOM and SALS.

The samples for TOM observation were prepared by pressing the melt between two pieces of cover glass with a thickness about 0.2 mm. The moment when the morphological structure appeared was defined as the phase separation time t_{ps}. Each t_{ps} at any particular temperature is the average of five tests with observation errors around ±3% as measured in various TP-modified TS systems.[17] The fact that the t_{ps} values are independent on the magnification of the TOM as shown in Table I proves that the onset of phase separation has been observed. If the initial domains were smaller than the resolution of the TOM system, one should see them earlier with higher magnification. The physical reason of limited initial size may be explained in view of the nature of spinodal decomposition as suggested by Inoue.[10] The initial fluctuation wavelength is a limit value and keeps almost constant with time becoming the periodic length of phase domains in the early stage of phase separation before domain growth driven by interfacial tension, so the early stage of the spinodal decomposition can be observed at similar t_{ps} using different TOM magnification.

SEM

The morphology of the fully cured blends was also examined with scanning electron microscopy (SEM

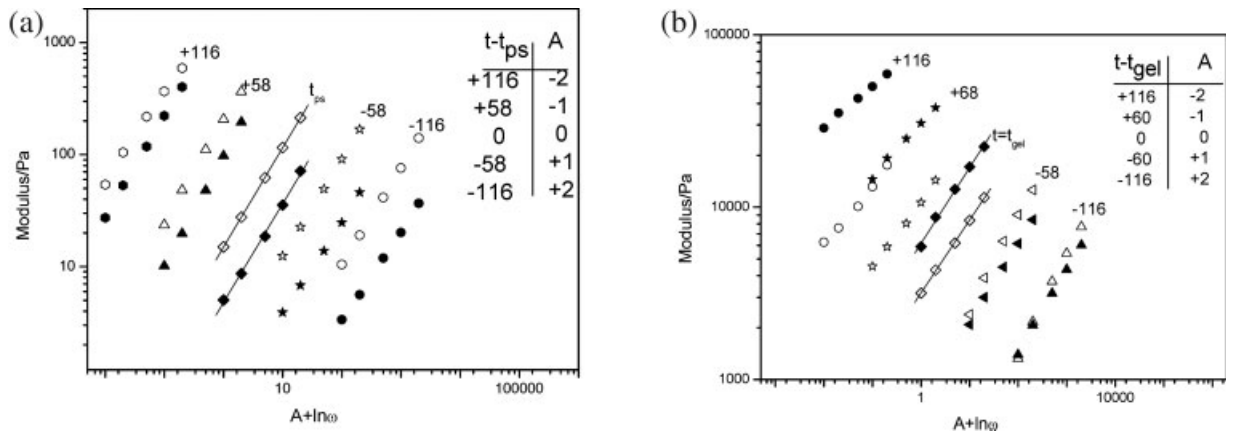

Figure 3 Frequency dependencies of G' (the solid symbols) and G'' (the open symbols) near (a) t_{ps} and (b) t_{gel} for epoxy/DDS/PEK-C 15 phr system curing at 170°C.

TABLE II
The Critical Relaxation Exponent Values of t_{ps} and t_{gel} at Different Temperature

T (°C)	t_{ps} (s)	n_{ps}	t_{gel} (s)	n_{gel}
150	2,162	0.86	3,959	0.40
160	1,565	0.85	2,567	0.40
170	1,005	0.88	1,655	0.43
180	602	0.89	1,197	0.45

Tescan Czech, model TS5136MM). The samples for SEM were cured at 170°C for 2 h and postcured at 200°C for 2 h. The cured samples were fractured in liquid nitrogen and coated with a layer of gold before observation. Before testing, etching was made by maintaining the specimens in tetrahydrofuran for 24 h.

DSC

A differential scanning calorimetric analysis was conducted using a Perkin–Elmer Pyris 1 instrument. The calorimeter was calibrated with high-purity indium and zinc standards. Dry nitrogen was used as purge gas with flow rate of 20 mL/min. The cure conversion, a, was determined on the basis of the following equation:

$$a = \frac{\Delta H_t}{\Delta H_\infty} \quad (1)$$

Here ΔH_t is the partial heat of reaction at time t or temperature T based on the results of the isothermal or dynamic heating test, ΔH_∞ is the average total heat of the reaction which was determined by total peak area of the dynamic DSC scans. The cure reaction rates was obtained by taking the derivative of a with respect to time or temperature.

RESULTS AND DISCUSSION

Phase separation observed on TOM

The epoxy/DDS/PEK-C mixture is a single phase system at the cure temperature (<LCST). As the cure reaction proceeded, some morphological structure appeared after an induction period as shown in Figure 2(a). The images show the onset of phase separation and the development of homogeneous domain size. The image contrast of the separated phases became stronger gradually with time, keeping the domain locus nearly fixed throughout the cure process. This feature is related to the low mobility of PEK-C with high M_w.

Rheological behaviors during cure process

Epoxy/DDS/PEK-C is a typical asymmetric mixture. PEK-C has much higher glass transition temperature (T_g = 221°C) and larger molar mass (M_w = 108,900). The cure conversion of the epoxy at the threshold of phase separation is about 24% as determined by isothermal DSC. The weight-average molar mass of the thermosetting resin is calculated to be about 2000, estimated using the recursive probability approach for crosslinking network formation developed by Macosko and Millerlb.[24] T_g for the thermosetting oligomers at phase separation threshold is about 40°C determined by DSC with a heating rate of 10°C/min. The large difference in T_g and molar mass of TS and TP are responsible for the dynamical asymmetry in the relaxation and diffusion of chain molecules which play a critical role in the phase separation process.[14,15]

Dynamic rheological measurement of epoxy/DDS/PEK-C blends with different PEK-C content were conducted at different isothermal temperature with multiple simultaneous frequencies, i.e., 1, 2, 5, 10, and 20 rad/s. Figure 2(a,b) shows the time varia-

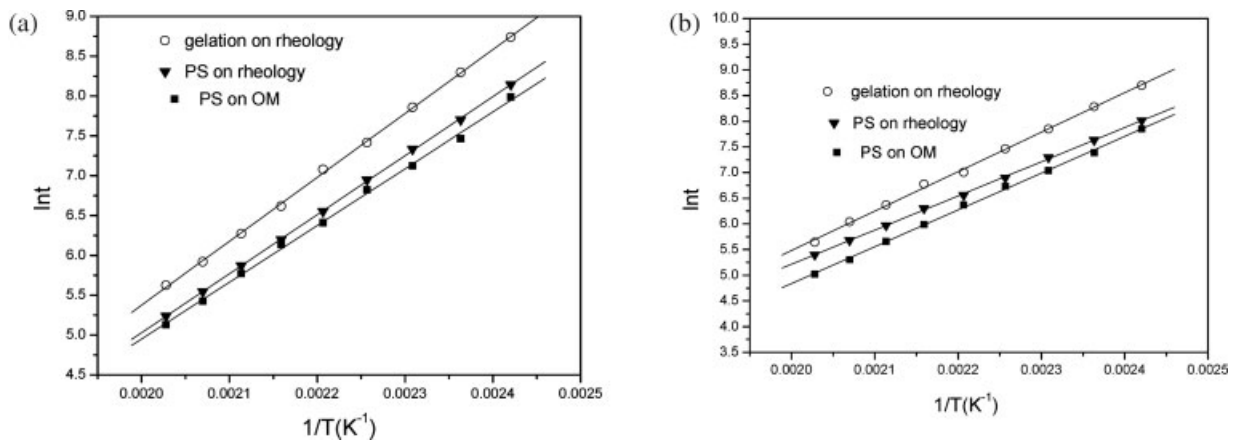

Figure 4 Arrhenius plots of the phase separation and gel time–temperature for epoxy/DDS systems with (a) 10 phr and (b) 15 phr PEK-C, respectively.

TABLE III
The Activation Energy Values of Phase Separation and Gelation for Epoxy/DDS/ PEK-C Systems

PEK-C content (phr)	E_a(ps, TOM) (kJ/mol)	R	E_a(ps, rheology) (kJ/mol)	R	E_a(gel, rheology) (kJ/mol)	R
10	59.8	0.999	62.1	0.999	67.2	0.997
15	60.0	0.999	55.8	0.999	66.4	0.999
20	57.5	0.998	61.2	0.999	67.2	0.999
30	60.5	0.999	63.4	0.997	68.1	0.994

tions of storage modulus G' and tangent loss angle tan δ at different frequencies for epoxy/DDS/PEK-C 15 phr system during curing at 170°C, together with the corresponding morphological optical micrographs.

At the beginning of cure, the blend has a storage modulus G' (in frequency of 10 rad/s) valued 13.4 Pa which changes exponentially up to the first-step growth at 991 s. TOM proved the appearance of the bicontinuous phase structure at the first transition. As the reaction proceeds, the shape of G' plots is further altered by the second rapid increase of G' at around 1752s, which corresponds to the chemical gelation of epoxy oligomers confirmed by solubility tests. After gelation, the contour of phase pattern is fixed and the margin of the domains became clearer gradually.

As shown in Figure 2(b), there are two kinetic transitions that are critical in the plots of tan δ at different frequencies. The curves cross at the time for phase separation t_{ps} and the time for chemical gelation t_{gel}, respectively, where loss tangent becomes independent of frequency, a typical attributes of critical gel state.[25] We will discuss such critical gel behaviors more systematically in the following section.

The critical gel behaviors at t_{ps} and t_{gel}

Corresponding to Figure 2(b), the storage modulus G' and the loss modulus G'' show scaling behaviors at both t_{ps} and t_{gel}[25] as follows:

$$G' \propto G'' \propto \omega^n \tag{2}$$

where ω is frequency and n is the critical relaxation exponent.

The evolution of linear viscoelastic properties, i.e., G' and G'' versus frequency in the vicinity of t_{ps} and t_{gel} for system of epoxy/DDS/PEK-C 15 phr isothermally curing at 170°C are displayed in Figure 3. The curves have been purposely shifted horizontally by a factor A (see insert) for easier comparison. The straight and parallel features of G' and G'' curves occur at both t_{ps} and t_{gel}, respectively. The scaling behavior extended over the entire experimental temperature range of 150–180°C. One of the difference between the critical gel at t_{ps} and t_{gel} is that G' is less than G'' at t_{ps} while larger than G'' at t_{gel} as shown in Figure 2(b) and also reported in other systems.[25] The second difference is in the slope of log G', G'' versus log ω curves at critical states.

The critical relaxation exponents at both t_{ps} and t_{gel} over temperature range of 150–180°C were calculated and tabulated in Table II.

By analyzing the data in Table II, it can be found that the relaxation exponent n values about 0.87 and 0.42 for t_{ps} and t_{gel}, respectively, are independent on temperatures. The n values fall in the range of 0.19–0.92 for many physical and chemical gel systems observed by other researchers.[25]

The existence of the constant n value for a critical gel is a signature of its self-similarity structure, for which the fractal geometry can be applied. Based on percolation theory, Muthukamar suggested that, the fractional dimension d_f can be represented in terms of relaxation exponent n[26] as follows:

$$d_f = \frac{(d+2)(d-2n)}{2(d-n)} \tag{3}$$

where d_f is the fractal dimension and d is the space dimension.

Taking the values of n_{ps}, n_{gel} (see Table II), and space dimension of 3 to eq. (3), we obtained the values of d_f which are valued about 1.48 for gel at t_{ps} and 2.1 for that at t_{gel}, respectively. A bigger n

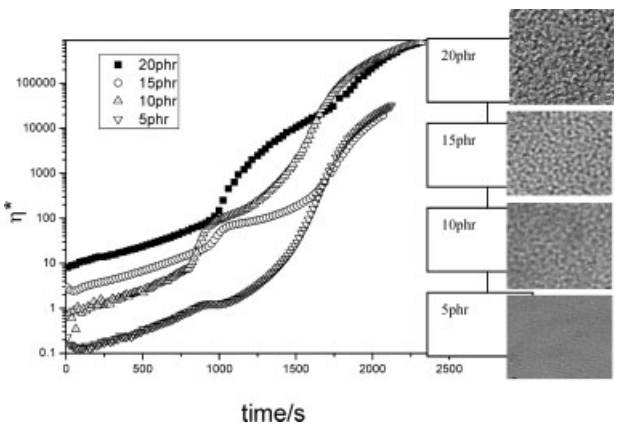

Figure 5 Effect of PEK-C content on η* and morphology for epoxy/DDS systems at 170°C.

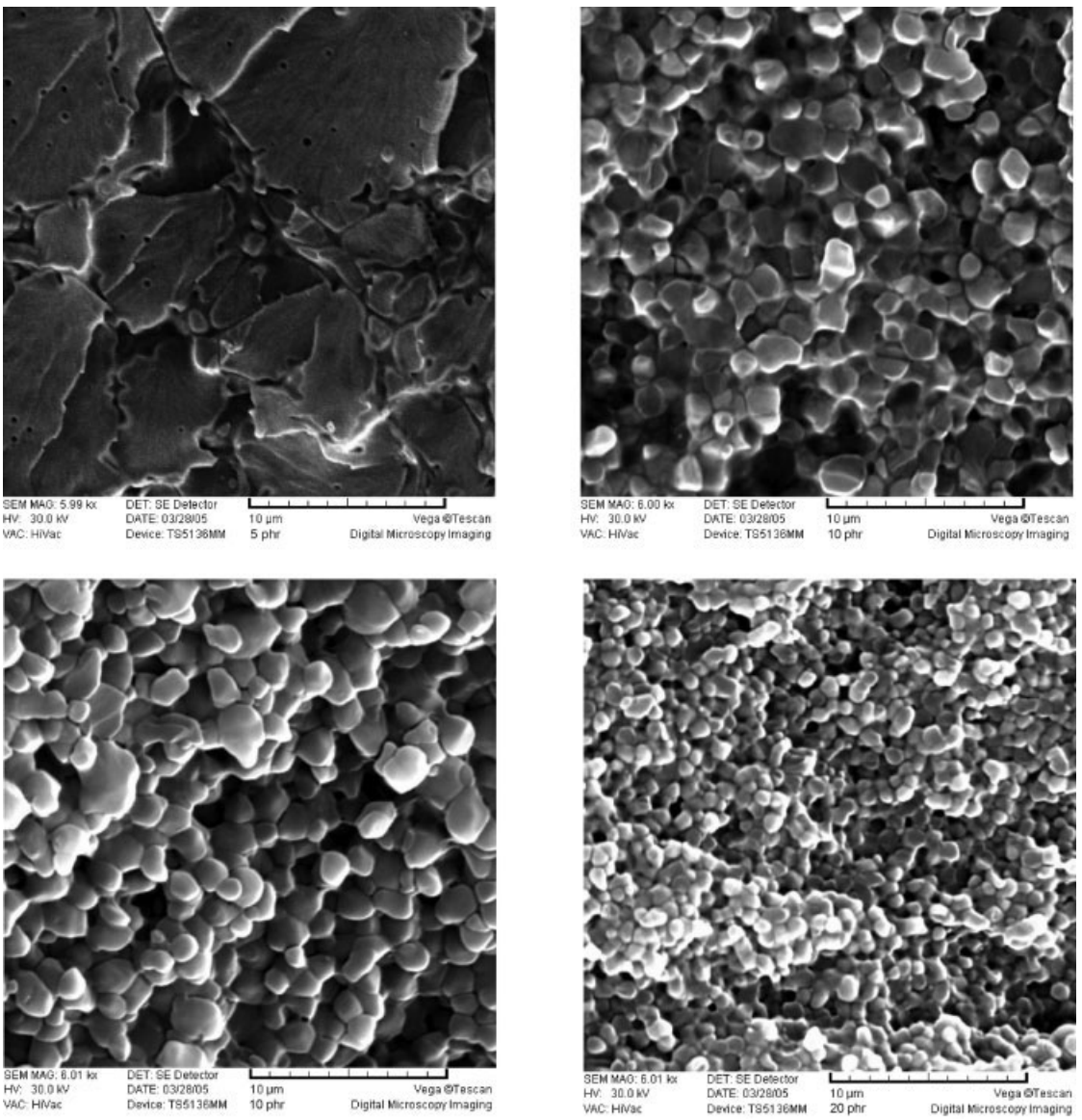

Figure 6 SEM micrographs for samples of epoxy/DDS/PEK-C with different PEK-C content.

means a looser network. This provides an insight into the morphology in Figure 2(a). The structure formed at t_{ps} is entangled long-chain TP polymers expelled by epoxy reaction which form a very sparse network yielding low fractal dimension d_f. The chemical gelation of epoxy with multifunctional crosslinker forms more compact network, thus, a bigger d_f value.

The time–temperature dependency of the phase separation and gelation

The phase separation time versus temperature data, based either on rheology or TOM, can be fit by the adaptation of the Arrhenius type equation (4) as follows:

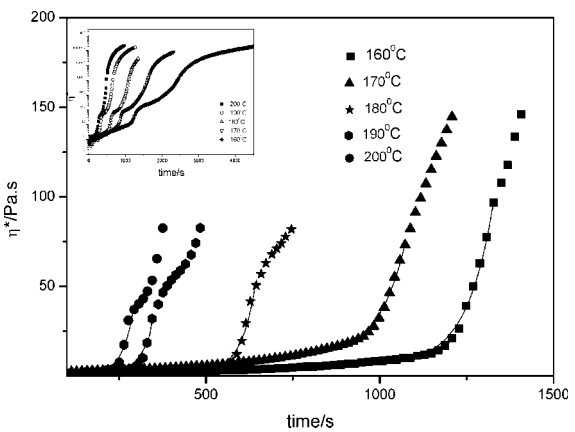

Figure 7 Viscosity—time profiles for isothermal cure of epoxy/DDS/PEK-C 10 phr at various temperatures.

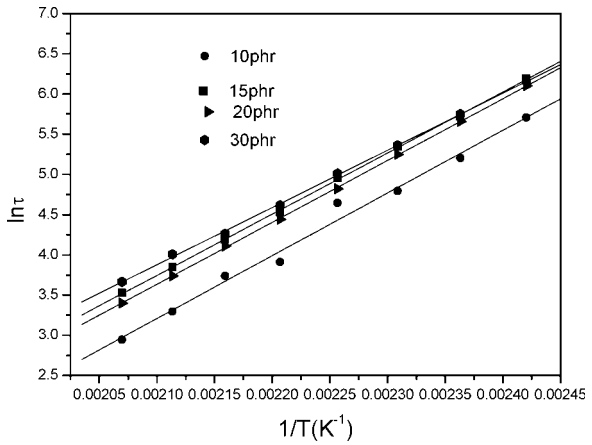

Figure 8 Effect of the PEK-C content on the relation of ln τ versus $1/T$.

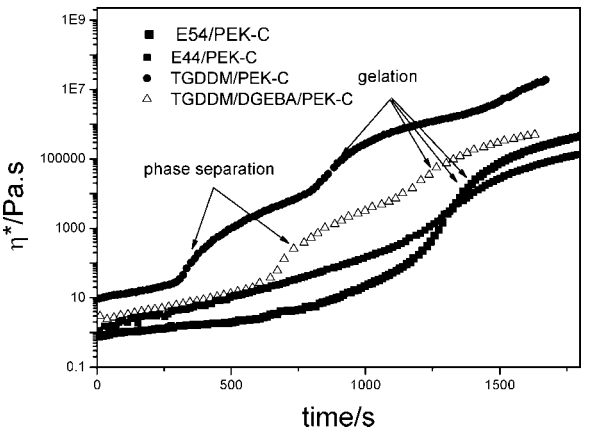

Figure 9 Change of complex viscosity for systems of epoxy/DDS/PEK-C 20 phr with different matrix formulations cure at 180°C.

$$\ln t_{\mathrm{ps}} = \ln k + \frac{E_a(\mathrm{ps})}{RT} \tag{4}$$

where t_{ps} is the phase separation time, E_a(ps) is the phase separation activation energy, T is the absolute temperature, and R is the universal gas constant.

Illustrated in Figure 4 are the experimental data of ln t_{ps} versus $1/T$ based on rheology and TOM for epoxy/DDS systems with 10 and 15 phr PEK-C, respectively, together with the plots for gel time/temperature. The corresponding activation energy derived from the slope of the plots is summarized in Table III.

As shown in Figure 4, the phase separation at all cure temperature occurs prior to chemical gelation of the thermosetting resin. The phase separation time t_{ps} (TOM) determined by TOM is earlier than that tested by rheology, since the former detects the appearing of optical inhomogeneity, while the later corresponds to the formation of percolated network. Yet, the parallel straight lines indicate similar activation energy by the two methods. The phase separation time/temperature, as well as the chemical gel time/temperature can be well described by Arrhenius equation (4).

The activation energy values listed in Table III indicate that systems with varying PEK-C contents present similar E_a(ps, TOM) and E_a(gel), respectively, in reasonable accuracy. The phase separation activation energy based on rheology E_a(ps, rheology) is slightly higher than E_a (ps, TOM) based on TOM. This is presumably due to the curing at tempering before rheology data collection at higher temperature. It took about 2 min after sample loaded for the plate temperature to be stabilized. We have compared E_a(ps) values for other systems based on TOM and light scattering and found agreement.[17]

Although E_a(ps) hardly changes with the PEK-C contents in the composition range of 5–30 phr, the morphology does change from island to bicontinuous or phase-inverted structure, and the rheology profiles also changed a lot correspondingly as shown in Figure 5. At the beginning of the cure, the homogeneous blends evolve almost linearly on the semilogarithmic sale. As cure proceeds, the complex viscosities η* increase in step growth in the vicinity of t_{ps}, depending on the morphology development in different compositions as observed by Pascault and coworkers[27] and Recca and coworkers[28] in other systems.

Figure 6 shows the SEM micrographs of the fully cured samples with different PEK-C content undergoing a cure schedule of 170°C for 2 h plus 200°C for 2 h. It can be seen that the sample with 5 phr PEK-C showed a fractured plain morphology and the addition of 10 phr or higher PEK-C lead to a connected granular morphology which is ascribed to

TABLE IV
E_a(ps) Based on Viscosity Growth and the Viscous Activation Energy E_η for Systems with Different PEK-C Content

PEK-C content (phr)	E_a(ps, viscosity growth) (kJ/mol)	R	E_η (kJ/mol)	R
10	64.8	0.994	26.0	0.998
15	63.2	0.999	26.3	0.999
20	63.9	0.999	23.8	0.997
30	59.1	0.999	25.1	0.996

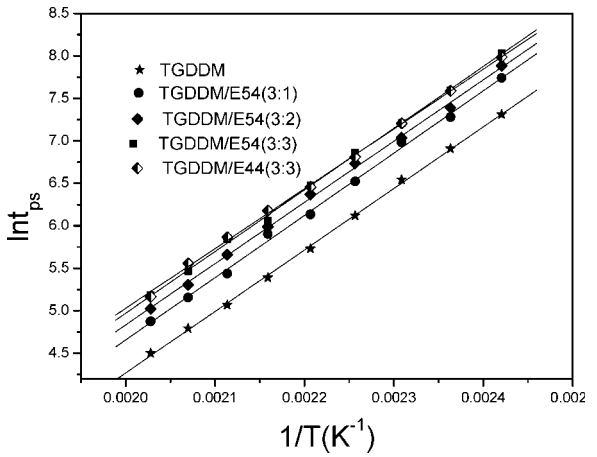

Figure 10 Plots of ln t_{ps} versus $1/T$ for epoxy/DDS/PEK-C 15 phr systems with different epoxy formulations (by TOM).

bicontinuous structure or phase-inverted structures, as noted by Inoue.[10] The size of phase domain is smaller at higher PEK-C content. It should be mentioned that the granular structures in SEM pictures appear partly due to the smoothing effect due to surface tension on swollen surface after solvent etching. This contributes the differences between SEM micrographs and TOM micrographs as shown in Figures 5 and 6.

The viscosity also changes along time and temperature as shown in Figure 7 for epoxy/DDS/PEK-C 10 phr system with the complete profiles shown on top left corner. The onset of the phase separation causes the viscosity to increase exponentially. Pascault and coworkers[27] and Recca and coworkers[28] noted similar behavior in other systems when phase separation appeared. The difference in our system is that we observed the morphology of the early stage of phase separation by TOM which shows a bicontinuous phase-separated structure upon phase separated appeared as shown in Figure 5 and then evolved into the phase-inverted structure as shown in Figure 6.

As expected, the higher the cure temperature, the earlier is the growth time of η^* due to phase separation. A Maxwellian type of relaxation function eq. (5) is used to correlate all the results as follows:

$$\eta^*(t) = \eta_0 \exp(t/\tau) \tag{5}$$

in which τ is the characteristic time, η_0 is initial complex viscosity, and t is cure time.

The good agreement as shown in Figure 7 supports the viscoelastic relaxation nature of phase separation. There are other equations to describe the viscosity evolvement prior to gelation,[27] but for the initial portion prior to phase separation, eq. (5) is sufficient and has the advantage to obtain the characteristic time of phase separation.

The characteristic times τ arising from eq. (5) under different temperatures were found to depend on temperature in an Arrhenius manner as follows:

$$\ln \tau = \ln \tau_0 + \frac{E_a}{RT} \tag{6}$$

Figure 8 proves this equation and yields the activation energy of phase separation E_a(ps, viscosity growth) shown in Table IV, which are similar to those of E_a(ps, rheology) arising from the critical gel criterion shown in Table III. Again systems with different PEK-C contents show similar phase separation activation energy.

Effect of epoxy monomers

The matrix formulations are changed by varying the mass ratio of TGDDM to E54, in some formulation E54 is replaced by E44. The viscosity profiles of the systems with different matrix formulations are very different as shown in Figure 9. The systems with the presence of TGDDM show double-step growth, while the systems without TGDDM show single-step growth at the threshold of chemical gelation. By TOM and SEM analysis, it was found that the systems without TGDDM show no phase-separated structure throughout the cure reaction.

The phase separation time/temperature dependence for systems with different matrix formulations are presented in Figure 10 and Table V. As shown

TABLE V
E_a(ps) Values of Epoxy/DDS/PEK-C 15 phr with Different Epoxy Formulation

Matrix	E_a(ps, TOM) (kJ/mol)	R	E_a(gel, rheology) (kJ/mol)	R	E_η (kJ/mol)	R
TGDDM	60.2	0.999	66.8	0.999	26.7	0.999
TGDDM/E54(3 : 1)	60.6	0.998	66.3	0.999	/	/
TGDDM/E54(3 : 2)	60.1	0.999	66.4	0.999	26.3	0.999
TGDDM/E54(3 : 3)	60.2	0.999	65.9	0.999	/	/
TGDDM/E44(3 : 3)	58.5	0.999	67.0	0.999	28.4	0.999
TGDDM/E54(no PEK-C)	/	/	67.1	0.999	26.1	0.999

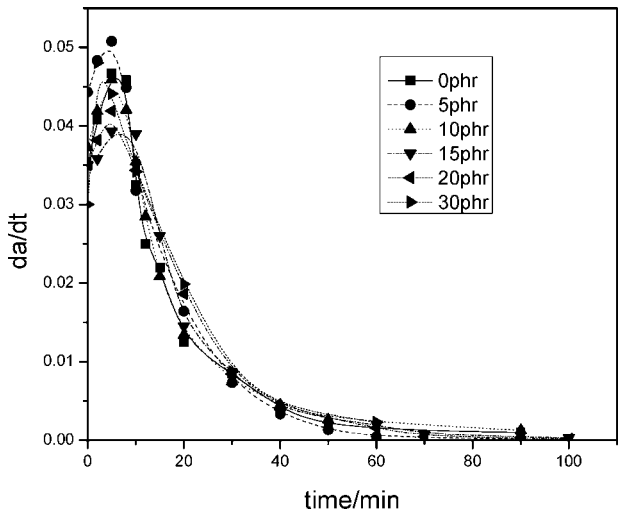

Figure 11 Plots of cure rate da/dt versus time for epoxy/DDS/PEK-C systems with different PEK-C contents at 180°C.

in Figure 10, the more TGDDM content, the earlier the phase separation takes place owing to the faster cure reaction. For instance, gel times cure at 170°C for systems E54/DDS, TGDDM/E54 (3 : 2)/DDS, TGDDM/DDS are 2525s, 1403s, 1075s, respectively. E_a(ps) in Table V for systems with different matrix formulation show similar values. The change of matrix resin has no obvious bearing on E_a(ps) in this system, although it will change the viscosity and epoxide concentration. At the same time, the miscibility of the components is expected to change along the matrix formulations for the fact that the systems without TGDDM show no phase separation upon cure, which indicate a better miscibility of the TS species with PEK-C component. We have found in other systems, e.g., DGEBA/DDM/PEI and DGEBA/DDM/PES, that E_a(ps) decreases with the increase of EEW of DGEBA monomers for the deteriorated miscibility reported by other researchers.[29,30]

The viscous activation energy E_η and cure activation energy E_a(gel) of systems with different matrix formulations are calculated and shown in Table V for later discussion.

The activation energies of viscous flow and cure reaction

It is interesting to check the viscous activation energy E_η and the cure activation energy E_a for systems with different PEK-C content and matrix formulations, since phase separation is a process driven by the free energy change for gelation reaction and realized through the molecular diffusion of small size TS species, which is also involved in the temperature dependence of viscous flow.

E_η is obtained from the initial viscosity of the homogeneous blends η_0 using Arrhenius form,[31] which is valid in the range far above the T_g of the blends. Plotting ln η_0 as function of $1/T$, the slope of these plots yields the required E_η listed in Tables IV and V for systems with different PEK-C contents and systems with different matrix formulations.

As for the PEK-C content is concerned, it seems that the values of E_η change little within tested epoxy oligomers and PEK-C loading levels, indicating the thermal motion of the epoxy oligomers is little bound by its detailed composition and PEK-C content in the present systems. The cure kinetics was analyzed by DSC technique. The cure rate versus time for systems with different PEK-C content is shown in Figure 11. The similar shape of the plots indicates that the increase of PEK-C content did not change the cure mechanism, although it may alter the cure rate. In other TP-incorporated systems, the cure rate may be changed as reported by Pascault

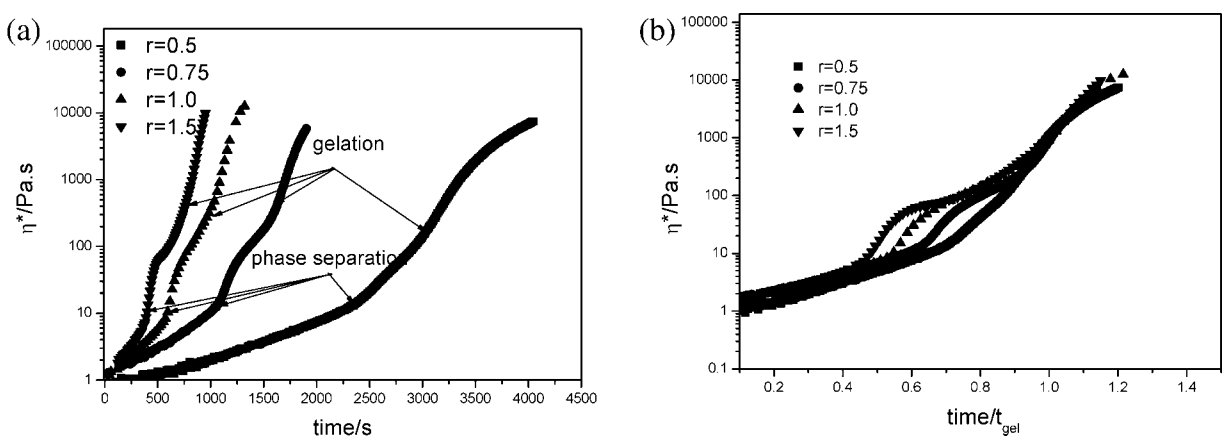

Figure 12 Effect of stoichiometric ratios on (a) complex viscosities versus time and (b) complex viscosities versus generalized time with t_{gel} of epoxy/DDS/PEK-C 15 phr systems at 180°C.

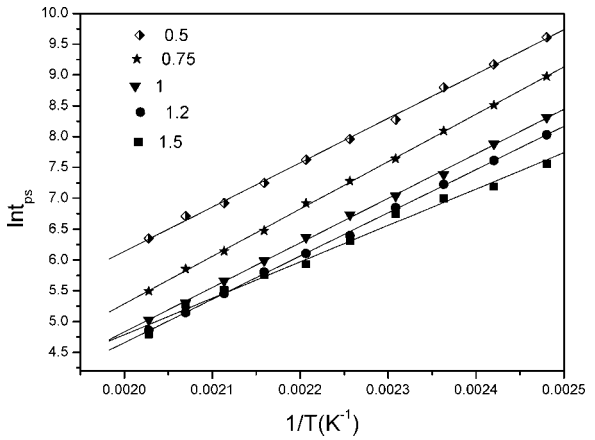

Figure 13 Plots of ln t_{ps} versus $1/T$ for epoxy/DDS/PEK-C15 phr systems with different stoichiometric ratios r (by TOM).

and coworkers[27] or unchanged as found by Su and Woo[32] and Yu et al.[15] Also, the cure activation energy may be elevated at high PEEK loading level beyond the practical range for toughening.[33] In this study, PEK-C loading level is limited up to 30 phr, the cure kinetics temperature dependence, i.e., the cure activation energy E_a(gel), as described in Table III, is found to be almost unchanged with increasing TP content. The fact that PEK-C content does not change E_η and E_a(gel) seems to be related to the independency of E_a(ps) on PEK-C content. Experiments in other systems shows that elevated E_a(gel) will yield higher E_a(ps).[17]

However, the correlation of E_η and E_a(ps) is complicated. We noticed in Table V that the system with E44 shows slightly higher E_η value but lower E_a(ps) indicating lower diffusion rate corresponding to easier phase separation. To understand this, we noticed the effect of miscibility, which would not affect much of the epoxy diffusion, but change the phase separation qualitatively. For example, the epoxy monomer with higher EEW generally shows deteriorated miscibility with the TP as reported by Bucknall et al.[29] and Bonnaud et al.[30] indicating higher EEW favors the phase separation process thus shows lower E_a(ps), but slightly higher E_η value. As a matter of fact, the dominant effect changing E_a(ps) is the interaction of TP and TS species or the chemical environment, which plays different role in E_a(ps) and E_η as we will discuss in the next section.

The effect of molar ratio of hardener/resin

The stoichiometric ratio of the system, r, is defined here as the molar ratio of amino hydrogen atoms to epoxy groups. Shown in Figure 12(a) are viscosity profiles of systems with different stoichiometric ratio cured at 180°C. It can been seen that the phase separation times of the system with stoichiometric or excess DDS content is greatly accelerated when compared with the systems with deficient DDS content, while the curve shape and the viscosity level at step growth arising from phase separation is quite similar for system with different stoichiometric ratios. Therefore, we were able to use reduced coordinate in Figure 12(b), where a general viscosity profiles versus reduced cure time t/t_{gel} may be obtained for all systems in Figure 12(a). They split at phase separation transition upon stoichiometric ratio: the phase separation times t_{ps} decrease with the increase of r value.

The phase separation time/temperature dependence of epoxy/DDS/PEK-C 15 phr system with different r value is summarized in Figure 13 and Table VI. As shown in Figure 13, the phase separation times are generally reduced with increasing r. The corresponding activation energy in Table VI shows that the phase separation activation energy based on rheology-E_a(ps, rheology) is higher than that based on TOM-E_a(ps, TOM) as was found in Table III, while both of them decrease with the increase of r. The characteristic time τ for systems with different stoichiometric ratio r at different temperatures was calculated based on eq. (5). Arrhenius equation (6) was employed to correlate the characteristic times τ and temperature, the fitting results are shown in Figure 14 and Table VII. It can be seen that the relaxation time increases as the DDS decrease, while the phase separation activation energy E_a(ps, viscosity growth) decease with the increase of r, which agrees with the results in Table VI.

By dynamic DSC analysis for neat resin/hardener systems with molar ratio of 0.5, 1, and 1.5 (see Fig. 15),

TABLE VI
E_a(ps) Values for Epoxy/DDS/PEK-C15 phr Systems with Different Stoichiometric Ratio r

r	E_a(ps, TOM) (kJ/mol)	R	E_a(ps, rheology) (kJ/mol)	R	E_a(gel, rheology) (kJ/mol)	R	E_a(DSC) (kJ/mol)	R
0.5	59.8	0.999	71.3	0.999	68.4	0.999	90.5	0.999
0.75	63.9	0.999	66.5	0.999	69.2	0.999	78.6	0.999
1	60.1	0.999	61.2	0.999	67.2	0.999	58.6	0.999
1.2	58.4	0.999	/	/	/	0.999	58.4	/
1.5	50.1	0.998	60.4	0.998	69.7	0.999	57.6	0.999

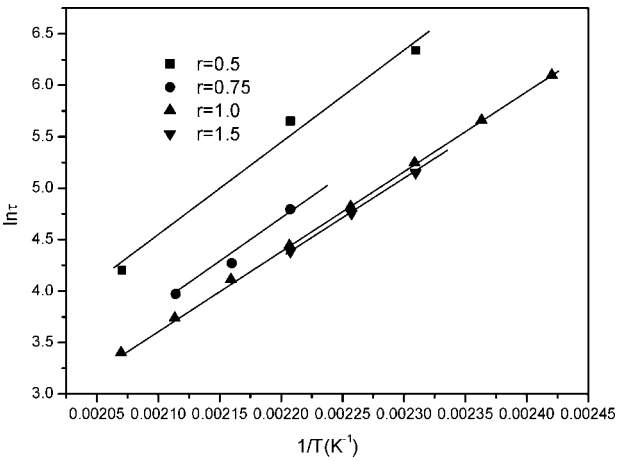

Figure 14 Effect of stoichiometric ratios r on the relation of ln τ versus $1/T$.

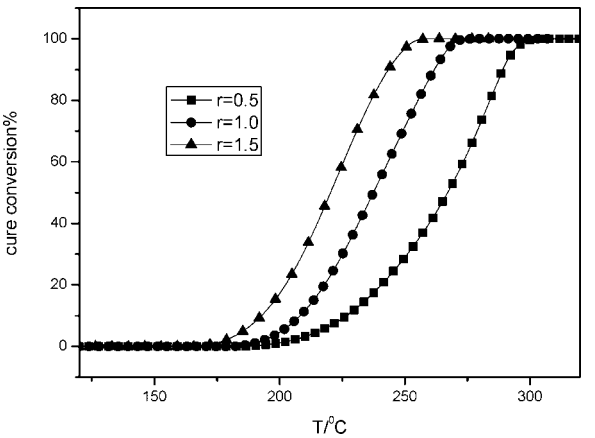

Figure 15 Cure conversions versus temperature plots for epoxy/DDS systems with different r at heating rate of 10°C/min.

it was found that the cure rate increases with r and in turn reduces the phase separation times.

The DSC curves scanned at different heating rates, i.e., 5, 10, 15, 20, and 25°C/min, allow the calculation of the activation energy of the overall curing reaction by the Kissinger method,[34] based on the equation derived from the condition for the maximum rate of the DSC curves:

$$E_a = -R^* \frac{d \ln(\beta/T_p^2)}{dT_p^{-1}} \quad (7)$$

where β is the heating rate, T_p is the peak temperature, E_a is the cure activation energy, and R is the gas constant.

The values of E_a for samples with different stoichiometric ratio r were calculated and tabulated in Table VI. It can be seen that the blends with deficiency r have high values of E_a which keeps almost constant when $r \geq 1$ as was found by other researchers.[35] The changing E_a for blends with deficient DDS may be ascribed to the etherification of epoxy in the later stage at high temperature as reported by other researchers.[36] The cure activation energy of systems with different DDS content was also calculated by Arrhenius fitting of the gel time–temperature detected by rheology and shown in Table VI with E_a(gel, rheology). It can be seen that E_a(gel, rheology) keeps unchanged with the variation of stoichiometric ratio indicating the etherification reaction has not yet occurred upon gelation. Since phase separation occurs prior to gelation, it is expected that the systems with different DDS contents have similar cure activation energy E_a(gel, rheology) contributing to the similar E_a(ps).

The viscous activation energy E_η for the systems with r of 0.5, 0.75, 1, and 1.5 are calculated and listed in Table VII. The value of E_η for system with the absence of DDS was also calculated for comparison. It can be seen that the systems with deficient DDS content shows a lower E_η value than the systems with stoichiometric or excess DDS contents. While the results in Table VI and Table VII show that the systems with higher DDS content present lower E_a(ps) value. Here, we see again the systems with higher E_η show lower E_a(ps). This is not surprising when we consider the miscibility effect. The reduction of E_a(ps) with increasing r presumably arises from the change of the miscibility of the components, i.e., the change of chemical environment by excess amine groups. The polar amine group is in favor of phase separation by lowering the energy barrier, E_a(ps).

TABLE VII
E_a(ps) Based on Viscosity Growth and the Viscous Activation Energy E_η for Systems with Different Stoichiometric Ratio

r	E_a(ps, viscosity growth) (kJ/mol)	R	E_η (kJ/mol)	R
0	/	/	17.6	0.999
0.5	74.9	0.998	16.7	0.998
0.75	73.7	0.999	17.6	0.999
1.0	63.9	0.999	26.3	0.997
1.5	62.4	0.999	26.1	0.996

CONCLUSIONS

The rheology and optical microscopic approaches enable us to characterize the phase separation transitions in processing time–temperature space on a TP/TS curing system of practical significance. The rheology profiles, i.e., modulus, viscosity versus time, show characteristic changes at t_{ps} and t_{gel}, respectively. The storage modulus G' and loss modulus G'' versus frequency curves at the thresholds of both phase separation and chemical gelation agree with the critical gel theory, showing lower fractal

dimension of the loose networking of the entangled thermoplastic polymer at t_{ps}, while a more compact fractal dimension at chemical gelation of TS. So, the critical gel analysis relates rheology to morphology during the cure process of PEK-C modified amine-cured epoxy systems, which were approved by the direct TOM observations.

The phase separation time of the TP/TS systems was determined and compared based on the rheological and morphological techniques. The phase separation time based on rheological criterion is slightly later than the phase separation time defined as the appearance of morphological structure under TOM observation, whereas both temperature dependencies of the phase separation times can be described by a common Arrhenius equation with similar phase separation activation energy E_a(ps). The universality of the Arrhenius equation in describing the phase separation time/temperature dependency has also been tested for other TP/TS systems recently.[17] The quantitative description of the time–temperature relations for phase separation and gelation provides more comprehensive framework in design the cure time/temperature paths for the processing of TP/TS blends. By adding the Arrhenius curve for phase separation to common used time–temperature-transformation (TTT) diagram one can better control and optimize the morphology and the final composite properties.

E_a(ps) values were analyzed in terms of PEK-C loading level, epoxy resin composition, and stoichiometric ratio of hardener. Rheology and TOM analysis showed that PEK-C loading level and epoxy composition in the tested range do change the viscosity and morphology at given temperatures, but do not alter E_a(sp), as well as the cure activation energy and viscous activation energy of the thermosetting species which are expected to play essential contribution to the values of E_a(sp) in the present systems. The decreasing of E_a(sp) with excess DDS is presumed to arise from the change of chemical environment due to excess amine groups. The systemic change of E_a(sp) with stoichiometric ratio was also found in other TP/TS blends. Further efforts should focus on finding the structural origin of ''chemical environment'' and its relations to the temperature dependency E_a(ps) of various TP/TS systems.

References

1. Browning, C. E. Polym Eng Sci 1978, 18, 16.
2. Morgan, R. J.; Mones, E. T. J Appl Polym Sci 1987, 33, 999.
3. Chiao, L. Macromolecules 1990, 23, 1286.
4. Bucknall, C. B.; Partridge, I. K. Polymer 1983, 24, 639.
5. Raghava, R. S. J Polym Sci Part B: Polym Phys 1987, 25, 1017.
6. Bucknall, C. B.; Gillbert, A. H. Polymer 1989, 30, 213.
7. Bennett, G. S.; Farris, R. J.; Thompson, S. A. Polymer 1991, 32, 1633.
8. Paul, D. R.; Bucknall, C. B. Polymer Blends: Formulations and Performance; Wiley: New York, 2000.
9. Tanaka, H. J Phys Condens Matter 2000, 12, R207.
10. Inoue, T. Prog Polym Sci 1995, 20, 119.
11. Girard-Reydet, E.; Sautereau, H.; Pascault, J. P.; Keates, P.; Navard, P; Thollet, G.; Vigier, G. Polrmer 1998, 39, 2269.
12. Riccardi, C. C.; Borrajo, J.; Williams, R. J. J.; Cirard-Reydet, E.; Sautereau, H.; Pascault, J. P. J Polym Sci Part B: Polym Phys 1996, 34, 349.
13. Williams, R. J. J.; Rozenberg, B. A.; Pascault, J. P. Adv Polym Sci 1997, 128, 97.
14. Gan, W. J.; Yu, Y. F.; Wang, M. H.; Tao, Q. S.; Li, S. J. Macromolecules 2003, 36, 7746.
15. Yu, Y. F.; Wang, M. H.; Gan, W. J.; Tao, Q. S.; Li, S. J. J Phys Chem B 2004, 108, 6208.
16. Simon, S. L.; Gillham, J. K. J Appl Polym Sci 1994, 53, 709.
17. Zhang, X. J.; Yi, X. S.; Xu, Y. Z. Acta Polym Sinica 2007, 725.
18. Zhang, X. J.; Xu, Y. Z. Advances in Rheology; Shangdong University Press: Jinan, 2006; p 138.
19. Zhang, H.; Chen, T.; Yuan, Y. Chin. Pat. 85,108,751 (1985).
20. Song, X. Z.; Zheng, S. X.; Huang, J. Y.; Zhu, P. P.; Guo, Q. P. J Appl Polym Sci 2001, 79, 598.
21. Guo, Q. P.; Huang, J. Y.; Li, B. Y.; Chen, T. L.; Zhang, H. F.; Feng, Z. L. Polymer 1991, 32, 58.
22. Tang, B. M.; An, X. F.; Yi, X. S. Mater Sci Forum 2005, 475–479, 1019.
23. Mours, M.; Winter, H. H. Rheol Acta 1994, 33, 385.
24. Macosko, C. W.; Millerlb, D. R. Macromolecules 1976, 9, 199.
25. Scanlan, J. C.; Winter, H. H. Macromolecules 1991, 24, 47.
26. Muthukumar, M. Macromolecules 1989, 22, 4656.
27. Bonnet, A.; Pascault, J. P.; Sautereau, Y. C. Macromolecules 1999, 32, 8524.
28. Blanco, I.; Cicala, G.; Motta, O.; Recca, A. J Appl Polym Sci 2004, 94, 361.
29. Bucknall, C. B.; Gomez, C. M.; Quintard, I. Polymer 1994, 35, 353.
30. Bonnaud, L.; Bonnet, A.; Pascault, J. P.; Sautereau, H.; Riccardi, C. C. J Appl Polym Sci 2002, 83, 1385.
31. Roller, M. B. Polym Eng Sci 1975, 15, 406.
32. Su, C. C.; Woo, E. M. Polymer 1995, 36, 2883.
33. Francis, B.; Poel, G. V.; Posada, F.; Groeninckx, G.; Rao, V. L.; Ramaswamy, R.; Thomas, S. Polymer 2003, 44, 3687.
34. Kissinger, H. E. Anal Chem 1957, 29, 702.
35. Yu, Y. F.; Cui, J.; Chen, W. J.; Li, S. J. Chem J Chin 1998, 19, 808.
36. Pyun, E.; Sook, C.; Sung, P. Macromolecules 1991, 24, 855.